

1
2
3
4
5
6
7
8
9
10 **Differential repositioning of the second transmembrane helices from *E. coli* Tar and EnvZ**
11 **upon moving the flanking aromatic residues**

12
13 Salomé C. Botelho^{1,a}, Karl Enquist^{1,b}, Gunnar von Heijne¹ and Roger R. Draheim^{*2,3}
14
15
16

17 ¹Department of Biochemistry and Biophysics, Stockholm University, Svante Arrhenius väg 16C,
18 SE-10691, Stockholm, Sweden; ²Division of Pharmacy and ³Wolfson Research Institute for Health
19 and Wellbeing, Durham University, Queen's Campus, Stockton-on-Tees, TS17 6BH, England,
20 United Kingdom
21

22 Current addresses: ^aDepartment of Molecular and Cellular Physiology, Howard Hughes Medical
23 Institute, Lorry Lokey SIM1 Building 07-535, 265 Campus Drive Room G1021, Stanford
24 University School of Medicine, Stanford, CA, 94305-5453, United States of America;
25 ^bOrganoClick AB, Ritar slingan 20, SE-18766, Täby, Sweden
26
27

28 Running title: Aromatic-based repositioning of Tar and EnvZ TM2
29
30
31
32
33
34
35
36

37 *To whom correspondence should be addressed (R. R. D.):
38
39

40 Durham University
41 Division of Pharmacy
42 Wolfson Building, Room F106
43 Stockton-on-Tees
44 TS17 6BH
45 England
46 United Kingdom
47 Tel: +44 191 334 0694
48 Fax: +44 191 334 0374
49 roger.draheim@durham.ac.uk
50
51

52 **Abstract**

53 Aromatic tuning, *i.e.* repositioning aromatic residues found at the cytoplasmic end of
54 transmembrane (TM) domains within bacterial receptors, has been previously shown to be an
55 efficient way to modulate signal output from the aspartate chemoreceptor (Tar) and the major
56 osmosensor EnvZ of *Escherichia coli*. In the case of Tar, changes in signal output consistent with
57 the vertical position of the native Trp-Tyr aromatic tandem within TM2 were observed. In contrast,
58 within EnvZ, where a Trp-Leu-Phe aromatic triplet was repositioned, the surface that the triplet
59 resided upon was shown to be the major determinant governing signal output. However, these
60 previous studies failed to determine whether moving the aromatic residues within TM2 of Tar or
61 EnvZ was sufficient to physically reposition the TM helix within a membrane. Recent coarse-
62 grained molecular dynamics (CG-MD) simulations predicted displacement of Tar TM2 upon
63 moving the aromatic residues at the cytoplasmic end of TM2. Here, we have employed a
64 glycosylation-mapping technique to demonstrate that repositioning the Trp-Tyr tandem within Tar
65 TM2 is sufficient to displace the C-terminal boundary of the helix relative to the membrane. In a
66 similar analysis of EnvZ, an abrupt initial displacement of TM2 was observed but no subsequent
67 movement was seen, suggesting that the vertical position of TM2 is not governed by the location of
68 the Trp-Leu-Phe triplet. In summary, our results support recent CG-MD simulations with
69 aromatically tuned Tar segments that demonstrated the Trp-Tyr tandem is sufficient to displace
70 TM2 within a membrane. Our results also provide another set of experimental data, *i.e.* the
71 resistance of EnvZ TM2 to being displaced upon aromatic tuning, which could be useful for
72 subsequent refinement of the initial CG-MD simulations. We suggest that differences observed
73 between the behavior of helices is due to the inherently different properties of the residues being
74 repositioned (*i.e.* Trp or Tyr versus Phe). Finally, we discuss the limitations of these methodologies,
75 how moving flanking aromatic residues might impact steady-state signal output and the potential to
76 employ aromatic tuning in other bacterial membrane-spanning receptors.

77 **Keywords**

78 Aromatic tuning / hydrophobic-polar membrane interface / interfacial anchoring / transmembrane
79 helices / glycosylation mapping

80

81

82 **Highlights**

- 83 • Aromatic tuning with a Trp-Tyr tandem displaces Tar TM2 in a membrane
- 84 • Displacement of Tar TM2 consistent with previous coarse grained molecular dynamics (CG-
85 MD) simulations
- 86 • Repositioning the Trp-Leu-Phe triplet does not incrementally displace EnvZ TM2
- 87 • Propensity for TM2 displacement agrees with previous patterns of tuned signal output

88

89

90 **Abbreviations**

91 WALP or YALP: α -helical peptides that possess an aliphatic core of Ala-Leu repeats flanked by
92 Trp (WALP) or Tyr (YALP) residues; TM: transmembrane; TM2: second transmembrane helix;
93 SHK: sensor histidine kinase; CG-MD: coarse-grained molecular dynamics; MGD: minimum
94 glycosylation distance; AS1: amphipathic sequence 1; AS2: amphipathic sequence 2, RM: rough
95 microsomes

96

98

99 Two-component signaling circuits allow bacteria to detect and respond to external stimuli.
100 However, for the majority of these circuits, the input stimulus remains unidentified. To circumvent
101 this limitation, we developed an “aromatic tuning” technique, *i.e.* repositioning the aromatic
102 residues commonly found at the cytoplasmic end of the transmembrane domain of receptors within
103 these circuits, to modulate steady-state signal output from the aspartate chemoreceptor (Tar) and
104 EnvZ, a major osmosensor, from *Escherichia coli* [1, 2]. In essence, aromatic tuning allows
105 stimulus-independent modulation of bacterial signaling circuits, which can be used to control
106 particular physiological or developmental processes without determination of the input stimulus.
107 Aromatic residues are conserved in similar locations in other receptors, suggesting that our tuning
108 approach could be applied to a wide variety of other two-component signaling circuits [3, 4].

109 Aromatic tuning was initially inspired by studies with α -helical peptides that possess an
110 aliphatic core of Ala-Leu repeats flanked by Trp (WALP) or Tyr (YALP) residues. These Trp and
111 Tyr residues demonstrated a distinct preference for the polar/hydrophobic interfaces between the
112 headgroups and acyl chains of synthetic lipid bilayers [5, 6]. Furthermore, a glycosylation-mapping
113 technique [7] highlighted the ability of Trp and Phe residues to reposition poly-Leu TM helices in
114 membranes due to their affinity for polar/hydrophobic interfaces [8]. Other studies have compared
115 the biophysical effects of having single or tandem aromatic residues at the end of these poly-Ala-
116 Leu α -helical peptides with respect to their preferred orientation and dynamics within different
117 synthetic bilayers [9, 10]. Therefore, substantial biochemical and biophysical evidence suggested
118 that repositioning the aromatic residues at the end of the TM2 helices would dramatically affect the
119 properties of these signaling helices and likely modulate signal output from membrane-spanning
120 receptors in which they were moved.

121

122 When we initially attempted aromatic tuning, the mechanistic models for transmembrane
123 signaling by Tar were based on piston-type displacements of TM2 [1, 4, 11-14]. We originally
124 hypothesized that aromatic tuning would displace TM2 of Tar within the membrane [1]. To
125 examine this hypothesis, a series of Tar receptors was created where the Trp-Tyr tandem found at
126 the cytoplasmic end of TM2 was moved up to three residue steps in either direction (Figure 1A). It
127 is important to note that Tar is not a canonical sensor histidine kinase (SHK), requires CheW and
128 CheA to form functional intracellular signaling complexes, and controls the direction of flagellar
129 rotation rather than gene transcription (Figure 1B) [15-18]. When these Tar receptors were
130 expressed within intact *E. coli* cells, an increase in steady-state signal output was observed that was
131 consistent with the vertical position of the aromatic residues within TM2 (Figure 1C) [1].

132 In order to determine whether aromatic tuning would work within a canonical SHK, we
133 examined its effectiveness using the major *E. coli* osmosensor, EnvZ, where a rotation of TM2 has
134 been proposed as the mechanism of transmembrane communication [19-23]. More recently,
135 regulated unfolding [24] and scissor-like models have been proposed for signaling by SHKs [25,
136 26]. Due to this variety of proposed mechanisms, we were unsure of what pattern of signal outputs
137 would be observed upon aromatic tuning. Within EnvZ, a Trp-Leu-Phe triplet was repositioned and
138 an anti-symmetrical fluorescent reporter system was employed to monitor steady-state signal
139 output. In this case, we observed that the surface of TM2 that the aromatic residues reside upon was
140 the major determinant in signal output rather than their vertical position (Figures 1D and 1E) [2].

141 In our previous studies, we did not directly demonstrate that moving the aromatic residues
142 within TM2 of Tar or EnvZ was sufficient to reposition either helix relative to the cytoplasmic
143 membrane [1, 2]. However, recent coarse-grained molecular dynamics (CG-MD) simulations
144 support displacement of Tar TM2 when aromatic tuning is employed [27]. Here, we utilize a
145 glycosylation-mapping technique to determine whether repositioning the aromatic residues is
146 sufficient to displace the membrane-embedded TM2 helices from Tar and EnvZ [7]. We

147 demonstrate that repositioning the aromatic residues, a Trp-Tyr tandem, that normally reside at the
148 cytoplasmic end of Tar TM2 resulted in a series of small incremental changes in minimal
149 glycosylation distance (MGD) consistent with repositioning the C-terminal boundary of the helix.
150 In the case of EnvZ, a Trp-Leu-Phe triplet was repositioned, and after an abrupt initial
151 displacement, no further substantial displacements were observed. We propose that this large initial
152 displacement is likely due to a loss of interaction between an arginyl residue and the membrane, and
153 that a pattern consistent with increasing TM2 displacement due to aromatic tuning was not
154 observed. We conclude by suggesting that differences observed between the behavior of helices is
155 due to the inherently different properties of the residues being repositioned (*i.e.* Trp or Tyr versus
156 Phe). We also discuss the limitations of these methodologies, how moving flanking aromatic
157 residues might impact steady-state signal output and the potential to employ aromatic tuning in
158 other bacterial membrane-spanning receptors.

159

160

161 2 *Materials and methods*

162

163 2.1 *Selection of residues comprising TM2 of Tar and EnvZ*

164

165 The primary sequences of Tar (GI: 16129838) and EnvZ (GI: 16131281) from *Escherichia*
166 *coli* K-12 MG1655 were subjected to a full protein scan with the ΔG predictor using a minimal
167 window of 9 residues and a maximal window of 40 residues [28]. This software searches the protein
168 sequences for putative TM helices by employing a sliding window of variable lengths and
169 calculating the ΔG_{app} for transmembrane insertion throughout the length of the sequence. In the case
170 of Tar, residues between Tyr-187 and Leu-217 were predicted to comprise TM2, while Leu-160 to
171 Ile-181 were proposed for EnvZ. In both cases, a motif commonly found within transmembrane

172 helices that consisted of positively charged residues and adjacent aromatic residues bracketing a core
173 of aliphatic residues was found within the predicted TM segments [29]. Based on this observation,
174 Arg-188 to Arg-213 from Tar and Arg-162 to Arg-180 from EnvZ were selected for glycosylation-
175 mapping analysis.

176

177 2.2 Glycosylation-mapping analysis

178

179 Model Lep proteins including the TM2 segments from Tar and EnvZ were expressed *in*
180 *vitro* from plasmid pGEM1 (Stratagene). To create the initial model Lep protein, the 5' end of the
181 *lepB* gene from *E. coli* was modified by the introduction of an *Xba*I site and by changing the
182 sequence 5' to the initiator ATG codon to a Kozak consensus sequence [30]. These proteins
183 contained one acceptor site for N-linked glycosylation in positions 3–5 (Asn-Ser-Thr; G1 in Figure
184 2A) included within an extended sequence of 24 residues (Met-Ala-Asn³-Ser-Thr-Ser-Gln-Gly-Ser-
185 Gln-Pro-Ile-Asn-Ala-Gln-Ala-Ala-Pro-Val-Ala-Gln-Gly-Gly-Ser-Gln-Gly-Glu-Phe⁵) inserted
186 between Asn³ and Phe⁵ in the wild-type sequence of Lep. A series of proteins that contained a
187 second acceptor site (Asn-Ser-Thr; G2 in Figure 2A) placed at single-residue increments between
188 positions 87-90 (d = 6 construct) and positions 92-94 (d = 11 construct) were created using standard
189 site-directed mutagenesis techniques (Stratagene). The predicted TM2 helices from either Tar or
190 EnvZ were introduced between an *Spe*I site in codons 60-61 and a *Kpn*I site in codon 80 of the *lepB*
191 gene using standard PCR amplification methods [31]. Plasmids pRD200 [4] or pEnvZ [32] or
192 served as templates for Tar or EnvZ, respectively. The oligonucleotides used during the
193 amplification introduced a flanking tetraresidyl sequence (Gly-Pro-Gly-Gly) to reduce the
194 propensity for formation of secondary structure that could alter the distance between the second
195 accepting site (G2) and the active site of OST [33]. Other Lep proteins were made by moving the

196 residues within TM2 of Tar (Trp-Tyr) or EnvZ (Trp-Leu-Phe) using standard site-directed
197 mutagenesis techniques (Stratagene) (Figures 3A and 4A).

198

199 2.3 *Expression in vitro and quantification of glycosylation*

200

201 The Lep proteins cloned in pGEM1 were transcribed and translated *in vitro* using the TNT
202 Quick Coupled Transcription/Translation System (Promega) as previously described [34]. Briefly, 1
203 µg of DNA template, 1 µL of ³⁵S-Met (5 µCi), and 0.5 µL of dog pancreas rough microsomes were
204 added at the start of the reaction, and samples were incubated for 90 min at 30 °C. To stop the
205 reaction, 40 µL of SDS sample buffer was added and the samples were incubated at 95 °C for 5
206 min, centrifuged for 2 min in a table-top microfuge (13000 x g) and 6 µL was loaded on a 10%
207 SDS/polyacrylamide gel. Translation products were analyzed by SDS-PAGE, and gels were
208 analyzed on a Fuji FLA-3000 PhosphorImager with the Image Reader v1.8J and Image Gauge
209 v4.22 software (Fujifilm). The extent of glycosylation was quantified with QtiPlot v0.9.7.5. To
210 calculate the percentage of doubly glycosylated (% 2X glycosylated), the quotient of the intensity of
211 the doubly glycosylated band to the summed intensities of the singly and doubly glycosylated bands
212 was calculated. The unglycosylated molecules that have not been targeted to the microsomes are
213 ignored but, in general, represent less than 25% of the total Lep present. In most cases, the
214 glycosylation efficiency varied by no more than 3 percent between different experiments.

215

216

217 3 *Results*

218

219 3.1 *Overview of glycosylation-mapping analysis*

220

221 Glycosylation-mapping analysis [7] was used to monitor changes in the position of TM2
222 segments within the membrane. This technique is based upon the ability of the lumenally located
223 endoplasmic reticulum enzyme oligosaccharyl transferase (OST) to add a glycan to the Asn residue
224 in Asn-Xaa-(Ser/Thr) glycosylation acceptor sites within target proteins. The Lep model protein we
225 used contains an N-terminal acceptor site for *N*-linked glycosylation (G1) to ensure that the analysis
226 includes only protein that becomes embedded within the microsomal membrane used in the assay
227 (Figure 2A). It also contains a second acceptor site (G2) that is incrementally moved further away
228 from the luminal face of the microsomal membrane. This movement allows the active site of OST
229 to act as a molecular ruler because each acceptor site will be glycosylated to an extent that
230 correlates with the distance between the active site of OST and the acceptor site (G2). In Figure 2A,
231 the red acceptor sites are not far enough from the luminal membrane to become glycosylated,
232 whereas the green sites are distal enough to become glycosylated. This technique was previously
233 used to measure the N- and C-terminal boundaries of several human α and β integrin subunits [35,
234 36]. The subsequent high-resolution structures of the transmembrane domains of α IIB monomer
235 [37], the β 3 monomer [38] and the α IIB β 3 heterodimer [39] confirmed these boundaries thereby
236 lending credence to glycosylation-mapping analysis. In addition, similar changes in the pattern of
237 glycosylation have been previously observed due to moving aromatic residues throughout the C-
238 terminal half of a poly-Leu transmembrane segment [8] suggesting that the technique is adequate
239 for detecting TM segment repositioning due to aromatic tuning.

240

241

242 3.2 *Baseline positions of TM2 from Tar and EnvZ*

243

244 Based on the previous success with determining TM boundaries by glycosylation mapping,
245 we performed similar studies with TM2 from Tar and EnvZ (Figure 2B). It should be noted that the

246 segments of interest are also flanked by two tetrapeptide sequences (Gly-Gly-Pro-Gly...Gly-Pro-
247 Gly-Gly) that serves to break secondary structure that could adversely affect comparisons between
248 different segments (Figure 2B). The Gly residue denoted with a +1 subscript in Figure 2B was
249 considered the first non-transmembrane residue. The percentage of unglycosylated, singly
250 glycosylated, and doubly glycosylated protein can be readily determined by SDS-PAGE because
251 the glycosylated forms of the protein migrate less rapidly (Figure 2C). We began by analyzing the
252 TM2 segment of Tar, and no glycosylation of G2 was observed when six ($d = 6$) or seven ($d = 7$)
253 residues were present between the boundary of the TM2 segment and G2. Moving G2 an additional
254 residue-step away from the membrane ($d = 8$) resulted in approximately 30% of the embedded Lep
255 protein undergoing two glycosylation events. Further movement of G2 away from the luminal
256 surface ($d \geq 9$) resulted in about 80% of total embedded protein becoming doubly glycosylated,
257 which approximates the maximal extent previously observed under these experimental conditions
258 (Figure 2C) [7]. To quantitatively compare TM segment position, the minimal glycosylation
259 distance (MGD), i.e., the number of residues required for half-maximal glycosylation (defined as
260 the value of d for which glycosylation efficiency is 40%), was calculated. For Tar TM2, the MGD
261 was determined to be 8.3 (Figure 2C).

262 The series of Lep proteins containing EnvZ TM2 exhibited no glycosylation of G2 when $d =$
263 6, 7 or 8. Repositioning G2 another residue away from the luminal surface resulted in about 60% of
264 the embedded Lep protein becoming doubly glycosylated. Moving the accepting site an additional
265 residue ($d = 10$) resulted in the previously observed maximal value of approximately 80% of the
266 embedded protein becoming doubly glycosylated [7]. For EnvZ TM2, the MGD was determined to
267 be 8.6 (Figure 2D). This increase in MGD indicates that more residues are required C-terminal to
268 the EnvZ TM2 segment in order to appropriately position the G2 acceptor site for glycosylation by
269 OST.

270

271

272 3.3 *TM2 of Tar is increasingly repositioned upon moving the Trp-Tyr tandem*

273

274 To monitor possible helix-repositioning effects due to aromatic tuning, a series of Lep
275 proteins containing segments in which the Trp-Tyr tandem was moved up to three residues toward
276 (minus-series) or away from (plus-series) the center of Tar TM2 were created (Figure 3A).
277 Subsequently, this series of Lep proteins was used as a template to create additional subsets that
278 contained a G2 acceptor site in single-residue increments from seven ($d = 7$) to ten ($d = 10$) residues
279 away from the luminal end of TM2. Creation of this library of Lep proteins allowed the
280 glycosylation-mapping assay described in Figure 2 to be performed on each tuned TM2 segment
281 from Tar (Figure 3A). Analysis of these aromatically tuned Tar segments resulted in trends similar
282 to the un-tuned version (Figure 2C). For each segment, the minimal extent of G2 glycosylation was
283 observed at $d = 7$ and the maximal extent at $d = 10$ (Figure 3B). During parallel analysis of the
284 aromatically tuned Tar variants, an MGD of 8.2 was observed for WY-3 through WY-1 segments
285 compared to the wild-type segment (WY 0) that possessed an MGD of 8.3. The WY+1 and WY+2
286 segments possessed MGDs of 8.6, while the WY+3 segment had an MGD of 8.7 (Figure 3B). We
287 previously demonstrated that employing aromatic tuning at the C-terminus of TM2 of Tar resulted
288 in incremental changes in steady-state signal output (Figure 1C) [1]. These glycosylation-mapping
289 results are consistent with repositioning of the cytoplasmic boundary of Tar TM2 during aromatic
290 tuning. However, other options such as a partial unwinding of the helix cannot be ruled out with this
291 methodology.

292

293

294 3.4 *TM2 of EnvZ remains more stationary upon moving the Trp-Leu-Phe triplet*

295

296 In a similar manner, a series of Lep proteins containing segments in which the Trp-Leu-Phe
297 triplet within EnvZ was moved up to three residues toward (minus-series) or away from (plus-
298 series) the center of TM2 were created. These were subsequently used as templates to create
299 additional subsets that contained a G2 acceptor site in single-residue increments from seven ($d = 7$)
300 to ten ($d = 10$) residues away from the luminal end of TM2 (Figure 4A). The MGD values
301 demonstrate that the C-terminus of the WLF-3 segment was displaced out of the membrane (MGD
302 = 7.9), while the other segments possessed MGDs ranging from 8.4 to 8.6 (Figure 4B). Analysis of
303 the EnvZ WLF+3 segment resulted in accumulation of a lower molecular weight product consistent
304 with cleavage of TM2 (presumably by the signal peptidase) from the Lep model protein [34]. Based
305 on this result, we did not analyze the segment any further. In the case of most EnvZ segments,
306 changes in MGD are small and not steadily increasing when compared to changes observed with
307 Tar, which suggests that an incremental repositioning of EnvZ TM2 does not occur. We suspect that
308 this abrupt transition is due to the Trp-Leu-Phe triplet repositioning the C-terminal boundary to
309 such an extent that the basic guanido group from the Arg side-chain can no longer interact with the
310 acidic phospholipid head groups (Figure 5). Arginyl side-chains have been shown to snorkel five to
311 six residues along a transmembrane helix [40] and it is possible that the WLF-3 segment is
312 displaced to such an extent that the Arg side-chain cannot contribute to the positioning of the C-
313 terminus [41].

314

315

316 4. Discussion

317

318 4.1 Differences in the initial position of TM2 helices and their subsequent repositioning

319

320 We have measured the minimum glycosylation distance (MGD) of TM2 segments from Tar and
321 EnvZ and observed that the segment from EnvZ is embedded slightly deeper into the membrane
322 than the counterpart from Tar, as observed by MGDs of 8.6 and 8.3, respectively. These results are
323 consistent with a previous study that demonstrated an inverse correlation between the length of a
324 poly-Leu TM segment and its relative MGD [7]. However, the difference in MGD for the TM2
325 segments (~ 0.3) is less than what would be expected for poly-Leu TM segments of similar lengths
326 (~ 1.5). This suggests that the affinity of the amphipathic aromatic residues (Trp and Tyr) for the
327 membrane interfacial region [5, 6, 8], the preference of Phe residues for the aliphatic membrane
328 core [8] and the interactions of the positively charged Arg residues with the negative
329 phospholipids [41] are also relevant in positioning of the TM2 segments within the membrane.

330 A previous study that employed comparative CG-MD simulations to examine the ability of
331 aromatic tuning to displace Tar TM2 in the presence of an explicit membrane and solvent
332 demonstrated that moving the Trp-Tyr residue was sufficient to induce small TM2 displacements of
333 up to 1.5 Å [27]. Assuming that the region in Lep that contains the G2 glycosylation site is in an
334 extended conformation, a shift in MGD of 0.5 residues as seen for the Tar constructs corresponds to
335 a shift in the positioning of the TM2 helix of 1.6-1.7 Å, close to the CG-MD results. It should also
336 be noted that the median value of the ensemble from all simulations is in agreement with our MGD
337 values for the aromatically tuned Tar TM2 helices. In both the CG-MD simulations and MGD
338 analysis, similar patterns of displacement were observed, *i.e.* a grouping of the minus-series of
339 receptors with similar displacements toward the cytoplasm (WY-3 through WY-1), a baseline
340 position for the wild-type (WY 0), two receptors that are slightly displaced toward the periplasm
341 (WY+1 and WY+2) and a larger shift toward the periplasm for the WY+3 variant (Figure 3). We
342 propose that the absence of EnvZ TM2 displacement should be comparatively assessed by CG-MD
343 simulation. In the case of EnvZ, moving the Trp-Leu-Phe triplet did not generate large changes in
344 MGD, with the exception of the WLF-3 variant, which could be due to the fact that the helix

345 displaced to such an extent that the Arg side-chain cannot contribute to the positioning of the C-
346 terminus [41].

347

348 *4.2 Limitations of an optimized single-helix approach during analysis of transmembrane* 349 *communication*

350

351 It is important to note that the context of TM2 within the full-length Tar and EnvZ receptors is
352 likely more complex than single independently acting α -helices. For example, within the CG-MD
353 simulations described above, contiguous optimized α -helices are explicitly forced [27]. Likewise,
354 within the glycosylation-mapping assay, the flanking tetrapeptide (Gly-Gly-Pro-Gly ... Gly-Pro-
355 Gly-Gly) is employed as a helix-breaker to ensure that all residues downstream are in an extended
356 form, however, the ability to prevent the membrane-embedded TM helix from partially unwinding
357 has not been probed [33]. Thus, when small fractional differences in MGD are observed, a partial
358 unwinding of the transmembrane helix cannot be explicitly ruled out.

359 Recently, a vast amount of structural, biochemical and genetic information has been
360 integrated into a “regulated unfolding” model of intraprotein signaling by SHKs [24]. This model
361 proposes that modular proteins are composed of individually folding domains that contribute
362 distinct functionalities to overall protein function. Within SHKs, the effector domain has been
363 suggested to be maintained in an inactive conformation by a rigid connection between the stimulus
364 perception and effector domains. Upon perception of stimulus, this structurally labile connection
365 would be disengaged in a manner that would allow the effector domain to adopt an active
366 conformation [24]. Previous biophysical analyses has demonstrated that the presence of tandem
367 amphipathic aromatic residues, Trp or Tyr, at one end of a transmembrane α -helix promotes
368 increased conformational dynamics compared to the presence of a single Trp or Tyr. This increase
369 has been proposed to be based upon the ability of the Trp and Tyr residues to form hydrogen bonds

370 with the polar head groups and interfacial water molecules. Consistent with these expectations, the
371 presence of two Phe residues is not remarkably different from a single Trp, Tyr or Phe residue [9,
372 10].

373 One intriguing possibility is that increased conformational dynamics at the cytoplasmic end
374 of TM2 could facilitate partial unwinding of the TM helix. Within intact bacterial membrane-
375 spanning receptors, the region connecting the TM to the HAMP domain is colloquially referred to
376 as a “control cable” because its residue composition governs coupling of signal transduction
377 between adjacent domains [1, 4, 42-49]. As proposed by the dynamic bundle of HAMP signal
378 transmission, this partial unwinding of the cytoplasmic end of TM2 could lead to destabilization of
379 AS1, the N-terminal helix within the HAMP domain, and thus to changes in AS2 and AS2' that
380 could subsequently be transmitted downstream to the domains responsible for signal output [42-44,
381 49]. Alternatively, within the context of the gearbox model, it is possible that a destabilization of
382 AS1 would lead to interconversion from knobs-to-knobs packing into a more canonical knobs-into-
383 holes packing and thus leading to downstream signaling [19-23]. Therefore, we hypothesize that the
384 Trp-209/Tyr-210 tandem in *E. coli* Tar maintains the baseline level of conformational dynamics at
385 the cytoplasmic end of TM2, such that a piston-type displacement of TM2 enhances interactions of
386 the aromatic tandem with the polar headgroups and interfacial waters to a degree that promotes
387 “regulated unfolding” of the membrane-adjacent HAMP domain. In the case of EnvZ, moving the
388 Trp-Leu-Phe, while clearly central to the concept of aromatic tuning, may not modulate dynamics at
389 the cytoplasmic end of TM2, as only a single amphipathic aromatic residue (Trp) exists in
390 conjunction with a largely hydrophobic residue (Phe) [9, 10].

391 From another slightly different, albeit interesting perspective, Trp-containing regions in
392 certain helical orientations have been shown to promote dimerization of Tar TM domains [50].
393 Therefore, moving the Trp residues may alter helix packing within Tar and EnvZ TM domains and
394 thus facilitate changes in the overall dynamic stability of the cytoplasmic end of the TM bundle.

395 Lending support to this concept is a study proposing that the presence of a water-filled hemi-
396 channel within the cytoplasmic end of the TM bundle is a critical component of signal transduction
397 within *E. coli* PhoQ [51]. It is possible that moving the aromatic residues around the surface of
398 TM2 results in certain positions where the aromatic residues would be positioned into this water-
399 filled hemi-channel, which could ultimately result in changes to PhoQ baseline signal output.
400 Therefore, it remains important to apply the optimized single-helix results presented here to the
401 greater complexities of transmembrane communication within the context of a full-length
402 membrane-spanning receptor.

403

404 4.3 *Wider adoption of aromatic tuning*

405

406 In our previous studies, we demonstrate the aromatic tuning results in changes in signal output from
407 both Tar and EnvZ, however, a difference in the pattern of signal outputs was observed (Figure 1)
408 [1, 2]. This pattern of signal outputs shows that even through aromatic tuning did not displace the
409 TM2 helix of EnvZ (Figure 4), it was still effective in modulating signal output within the full-
410 length receptor. In that regard, we suggest that aromatic tuning was able to achieve its initial goal of
411 stimulus-independent modulation of a two-component signaling circuit. Published sequence
412 alignments have shown that aromatic residues are often found at the cytoplasmic end of the final
413 transmembrane helix within bacterial membrane-spanning receptors [3, 4] suggesting that aromatic
414 tuning will be useful for other research groups working with other two-component circuits. We
415 hope that these results, in conjunction with our previous demonstration of the differences in α -
416 helicity of AS1 segments [52], promote continued discussion about the mechanisms of
417 transmembrane communication within bacterial membrane-spanning receptors.

418

419

420 **Acknowledgments**

421

422 Members of the von Heijne group provided valuable support and discussion during the early stages
423 of the manuscript. S. C. B. was supported by a graduate student fellowship (SFRH/BD/26017/2007)
424 from Fundação para a Ciência e a Tecnologia, Portugal. This work was also supported by grants
425 from the Swedish Foundation for Strategic Research, the Swedish Research Council and the
426 Swedish Cancer Foundation to G. v. H. A Kirschstein National Research Service Award from the
427 National Institutes of Health (AI075573) supported R. R. D. during the initial phases of this work.

428

429

430 **References**

431

- 432 [1] R.R. Draheim, A.F. Bormans, R.Z. Lai, M.D. Manson, Tuning a bacterial chemoreceptor with
433 protein-membrane interactions, *Biochemistry*, 45 (2006) 14655-14664.
- 434 [2] M.H. Norholm, G. von Heijne, R.R. Draheim, 'Forcing the issue' - Aromatic tuning facilitates
435 stimulus-independent modulation of a two-component signaling circuit, (2014) *ACS Synth Biol*
- 436 [3] T. Boldog, G.L. Hazelbauer, Accessibility of introduced cysteines in chemoreceptor
437 transmembrane helices reveals boundaries interior to bracketing charged residues, *Protein Sci*, 13
438 (2004) 1466-1475.
- 439 [4] R.R. Draheim, A.F. Bormans, R.Z. Lai, M.D. Manson, Tryptophan residues flanking the second
440 transmembrane helix (TM2) set the signaling state of the Tar chemoreceptor, *Biochemistry*, 44
441 (2005) 1268-1277.
- 442 [5] J.A. Killian, I. Salemink, M.R. de Planque, G. Lindblom, R.E. Koeppe, 2nd, D.V. Greathouse,
443 Induction of nonbilayer structures in diacylphosphatidylcholine model membranes by
444 transmembrane alpha-helical peptides: importance of hydrophobic mismatch and proposed role of
445 tryptophans, *Biochemistry*, 35 (1996) 1037-1045.
- 446 [6] M.R. de Planque, J.W. Boots, D.T. Rijkers, R.M. Liskamp, D.V. Greathouse, J.A. Killian, The
447 effects of hydrophobic mismatch between phosphatidylcholine bilayers and transmembrane alpha-
448 helical peptides depend on the nature of interfacially exposed aromatic and charged residues,
449 *Biochemistry*, 41 (2002) 8396-8404.
- 450 [7] I. Nilsson, A. Saaf, P. Whitley, G. Gafvelin, C. Waller, G. von Heijne, Proline-induced
451 disruption of a transmembrane alpha-helix in its natural environment, *J Mol Biol*, 284 (1998) 1165-
452 1175.
- 453 [8] P. Braun, G. von Heijne, The aromatic residues Trp and Phe have different effects on the
454 positioning of a transmembrane helix in the microsomal membrane, *Biochemistry*, 38 (1999) 9778-
455 9782.

456 [9] N.J. Gleason, V.V. Vostrikov, D.V. Greathouse, C.V. Grant, S.J. Opella, R.E. Koeppe, 2nd,
457 Tyrosine replacing tryptophan as an anchor in GWALP peptides, *Biochemistry*, 51 (2012) 2044-
458 2053.

459 [10] K.A. Sparks, N.J. Gleason, R. Gist, R. Langston, D.V. Greathouse, R.E. Koeppe, 2nd,
460 Comparisons of interfacial Phe, Tyr, and Trp residues as determinants of orientation and dynamics
461 for GWALP transmembrane peptides, *Biochemistry*, 53 (2014) 3637-3645.

462 [11] J.J. Falke, A.H. Erbse, The piston rises again, *Structure*, 17 (2009) 1149-1151.

463 [12] J.J. Falke, G.L. Hazelbauer, Transmembrane signaling in bacterial chemoreceptors, *Trends in*
464 *biochemical sciences*, 26 (2001) 257-265.

465 [13] A.S. Miller, J.J. Falke, Side chains at the membrane-water interface modulate the signaling
466 state of a transmembrane receptor, *Biochemistry*, 43 (2004) 1763-1770.

467 [14] B. Isaac, G.J. Gallagher, Y.S. Balazs, L.K. Thompson, Site-directed rotational resonance solid-
468 state NMR distance measurements probe structure and mechanism in the transmembrane domain of
469 the serine bacterial chemoreceptor, *Biochemistry*, 41 (2002) 3025-3036.

470 [15] M. Welch, K. Oosawa, S. Aizawa, M. Eisenbach, Phosphorylation-dependent binding of a
471 signal molecule to the flagellar switch of bacteria, *Proc Natl Acad Sci U S A*, 90 (1993) 8787-8791.

472 [16] S. Ravid, P. Matsumura, M. Eisenbach, Restoration of flagellar clockwise rotation in bacterial
473 envelopes by insertion of the chemotaxis protein CheY, *Proc Natl Acad Sci U S A*, 83 (1986) 7157-
474 7161.

475 [17] J.F. Hess, K. Oosawa, N. Kaplan, M.I. Simon, Phosphorylation of three proteins in the
476 signaling pathway of bacterial chemotaxis, *Cell*, 53 (1988) 79-87.

477 [18] K.A. Borkovich, N. Kaplan, J.F. Hess, M.I. Simon, Transmembrane signal transduction in
478 bacterial chemotaxis involves ligand-dependent activation of phosphate group transfer, *Proc Natl*
479 *Acad Sci U S A*, 86 (1989) 1208-1212.

480 [19] H.U. Ferris, K. Zeth, M. Hulko, S. Dunin-Horkawicz, A.N. Lupas, Axial helix rotation as a
481 mechanism for signal regulation inferred from the crystallographic analysis of the *E. coli* serine
482 chemoreceptor, *J Struct Biol*, 186 (2014) 349-356.

483 [20] H.U. Ferris, S. Dunin-Horkawicz, L.G. Mondejar, M. Hulko, K. Hantke, J. Martin, J.E.
484 Schultz, K. Zeth, A.N. Lupas, M. Coles, The mechanisms of HAMP-mediated signaling in
485 transmembrane receptors, *Structure*, 19 (2011) 378-385.

486 [21] H.U. Ferris, S. Dunin-Horkawicz, N. Hornig, M. Hulko, J. Martin, J.E. Schultz, K. Zeth, A.N.
487 Lupas, M. Coles, Mechanism of regulation of receptor histidine kinases, *Structure*, 20 (2012) 56-66.

488 [22] M. Hulko, F. Berndt, M. Gruber, J.U. Linder, V. Truffault, A. Schultz, J. Martin, J.E. Schultz,
489 A.N. Lupas, M. Coles, The HAMP domain structure implies helix rotation in transmembrane
490 signaling, *Cell*, 126 (2006) 929-940.

491 [23] M. Inouye, Signaling by transmembrane proteins shifts gears, *Cell*, 126 (2006) 829-831.

492 [24] J.E. Schultz, J. Natarajan, Regulated unfolding: a basic principle of intraprotein signaling in
493 modular proteins, *Trends in biochemical sciences*, 38 (2013) 538-545.

494 [25] J.J. Falke, Piston versus Scissors: Chemotaxis Receptors versus Sensor His-Kinase Receptors
495 in Two-Component Signaling Pathways, *Structure*, 22 (2014) 1219-1220.

496 [26] K.S. Molnar, M. Bonomi, R. Pellarin, G.D. Clinthorne, G. Gonzalez, S.D. Goldberg, M.
497 Goulian, A. Sali, W.F. DeGrado, Cys-Scanning Disulfide Crosslinking and Bayesian Modeling
498 Probe the Transmembrane Signaling Mechanism of the Histidine Kinase, PhoQ, *Structure*, 22
499 (2014) 1239-1251.

500 [27] B.A. Hall, J.P. Armitage, M.S.P. Sansom, Transmembrane Helix Dynamics of Bacterial
501 Chemoreceptors Supports a Piston Model of Signalling, *PLoS Comput Biol*, 7 (2011) e1002204.

502 [28] T. Hessa, N.M. Meindl-Beinker, A. Bernsel, H. Kim, Y. Sato, M. Lerch-Bader, I. Nilsson, S.H.
503 White, G. von Heijne, Molecular code for transmembrane-helix recognition by the Sec61
504 translocon, *Nature*, 450 (2007) 1026-1030.

505 [29] T.K. Nyholm, S. Ozdirekcan, J.A. Killian, How protein transmembrane segments sense the
506 lipid environment, *Biochemistry*, 46 (2007) 1457-1465.

507 [30] M. Kozak, Initiation of translation in prokaryotes and eukaryotes, *Gene*, 234 (1999) 187-208.

508 [31] A. Saaf, E. Wallin, G. von Heijne, Stop-transfer function of pseudo-random amino acid
509 segments during translocation across prokaryotic and eukaryotic membranes, *Eur J Biochem*, 251
510 (1998) 821-829.

511 [32] W. Hsing, T.J. Silhavy, Function of conserved histidine-243 in phosphatase activity of EnvZ,
512 the sensor for porin osmoregulation in *Escherichia coli*, *J Bacteriol*, 179 (1997) 3729-3735.

513 [33] T. Hessa, H. Kim, K. Bihlmaier, C. Lundin, J. Boekel, H. Andersson, I. Nilsson, S.H. White,
514 G. von Heijne, Recognition of transmembrane helices by the endoplasmic reticulum translocon,
515 *Nature*, 433 (2005) 377-381.

516 [34] C. Lundin, H. Kim, I. Nilsson, S.H. White, G. von Heijne, Molecular code for protein insertion
517 in the endoplasmic reticulum membrane is similar for N(in)-C(out) and N(out)-C(in)
518 transmembrane helices, *Proc Natl Acad Sci U S A*, 105 (2008) 15702-15707.

519 [35] A. Stefansson, A. Armulik, I. Nilsson, G. von Heijne, S. Johansson, Determination of N- and
520 C-terminal borders of the transmembrane domain of integrin subunits, *J Biol Chem*, 279 (2004)
521 21200-21205.

522 [36] A. Armulik, I. Nilsson, G. von Heijne, S. Johansson, Determination of the border between the
523 transmembrane and cytoplasmic domains of human integrin subunits, *J Biol Chem*, 274 (1999)
524 37030-37034.

525 [37] T.L. Lau, V. Dua, T.S. Ulmer, Structure of the integrin alphaIIb transmembrane segment, *J*
526 *Biol Chem*, 283 (2008) 16162-16168.

527 [38] T.L. Lau, A.W. Partridge, M.H. Ginsberg, T.S. Ulmer, Structure of the integrin beta3
528 transmembrane segment in phospholipid bicelles and detergent micelles, *Biochemistry*, 47 (2008)
529 4008-4016.

530 [39] T.L. Lau, C. Kim, M.H. Ginsberg, T.S. Ulmer, The structure of the integrin alphaIIbbeta3
531 transmembrane complex explains integrin transmembrane signalling, *EMBO J*, 28 (2009) 1351-
532 1361.

533 [40] D. Stopar, R.B. Spruijt, C.J. Wolfs, M.A. Hemminga, Local dynamics of the M13 major coat
534 protein in different membrane-mimicking systems, *Biochemistry*, 35 (1996) 15467-15473.

535 [41] M. Monne, I. Nilsson, M. Johansson, N. Elmhed, G. von Heijne, Positively and negatively
536 charged residues have different effects on the position in the membrane of a model transmembrane
537 helix, *J Mol Biol*, 284 (1998) 1177-1183.

538 [42] J.S. Parkinson, Signaling mechanisms of HAMP domains in chemoreceptors and sensor
539 kinases, *Annu Rev Microbiol*, 64 (2010) 101-122.

540 [43] Q. Zhou, P. Ames, J.S. Parkinson, Biphasic Control Logic of HAMP Domain Signaling in the
541 *Escherichia coli* Serine Chemoreceptor, *Mol Microbiol*, (2011).

542 [44] S. Kitanovic, P. Ames, J.S. Parkinson, Mutational analysis of the control cable that mediates
543 transmembrane signaling in the *Escherichia coli* serine chemoreceptor, *J Bacteriol*, 193 (2011)
544 5062-5072.

545 [45] H. Park, W. Im, C. Seok, Transmembrane signaling of chemotaxis receptor tar: insights from
546 molecular dynamics simulation studies, *Biophys J*, 100 (2011) 2955-2963.

547 [46] G.A. Wright, R.L. Crowder, R.R. Draheim, M.D. Manson, Mutational analysis of the
548 transmembrane helix 2-HAMP domain connection in the *Escherichia coli* aspartate chemoreceptor
549 tar, *J Bacteriol*, 193 (2011) 82-90.

550 [47] C.A. Adase, R.R. Draheim, G. Rueda, R. Desai, M.D. Manson, Residues at the cytoplasmic
551 end of transmembrane helix 2 determine the signal output of the TarEc chemoreceptor,
552 *Biochemistry*, 52 (2013) 2729-2738.

553 [48] C.A. Adase, R.R. Draheim, M.D. Manson, The residue composition of the aromatic anchor of
554 the second transmembrane helix determines the signaling properties of the aspartate/maltose
555 chemoreceptor Tar of *Escherichia coli*, *Biochemistry*, 51 (2012) 1925-1932.
556 [49] Q. Zhou, P. Ames, J.S. Parkinson, Mutational analyses of HAMP helices suggest a dynamic
557 bundle model of input-output signalling in chemoreceptors, *Mol Microbiol*, 73 (2009) 801-814.
558 [50] N. Sal-Man, D. Gerber, I. Bloch, Y. Shai, Specificity in transmembrane helix-helix interactions
559 mediated by aromatic residues, *J Biol Chem*, 282 (2007) 19753-19761.
560 [51] S.D. Goldberg, G.D. Clinthorne, M. Goulian, W.F. DeGrado, Transmembrane polar
561 interactions are required for signaling in the *Escherichia coli* sensor kinase PhoQ, *Proc Natl Acad*
562 *Sci U S A*, 107 (2010) 8141-8146.
563 [52] S. Unnerstale, L. Maler, R.R. Draheim, Structural characterization of AS1-membrane
564 interactions from a subset of HAMP domains, *Biochim Biophys Acta*, 1808 (2011) 2403-2412.
565 [53] M. Kollmann, L. Lovdok, K. Bartholome, J. Timmer, V. Sourjik, Design principles of a
566 bacterial signalling network, *Nature*, 438 (2005) 504-507.
567 [54] P. Cluzel, M. Surette, S. Leibler, An ultrasensitive bacterial motor revealed by monitoring
568 signaling proteins in single cells, *Science*, 287 (2000) 1652-1655.
569

570

571 **Figure legends**

572

573 Figure 1. Synopsis of results from aromatic tuning of Tar and EnvZ TM2. (A) Within Tar TM2, a
574 Trp-Tyr (red) was moved about its original position at the cytoplasmic polar/hydrophobic interface
575 [1]. (B) The chemotactic circuit of *E. coli* [53]. Chemotaxis proteins are denoted by a single letter,
576 e.g. CheR denoted as “R”, and the activated form of Tar is indicated with an asterisk (Tar*).
577 Aspartate (Asp) binds to Tar and promotes the inactive form, which results in decreased
578 intracellular levels of CheY-P. The intracellular level of CheY-P governs the probability of
579 clockwise flagellar rotation (P_{CW}) [54]. (C) Rotation of a single flagellum from roughly 200
580 independent cells expressing one of the aromatically tuned variants were analyzed for 30 seconds
581 and classified into one of five categories (left to right): rotating exclusively CCW, rotating mostly
582 CCW with occasional reversals, rapidly switching between both rotational directions (CW/CCW),
583 rotating mostly CW with occasional reversals and rotating exclusively CW. As P_{CW} increases, the
584 number of cells in each category shifts from the left end of the axis toward the right end. In
585 summary, the lowest overall P_{CW} was observed from cells expressing the WY-3 variant, while the

586 greatest was observed from cells expressing the WY+2 or WY+3 variants. In the case of Tar, the
587 vertical position of the aromatic residues correlates with P_{CW} [1]. (D) When aromatic tuning was
588 performed in EnvZ, a Trp-Leu-Phe triplet (red) was repositioned [2]. (E) The EnvZ/OmpR
589 osmosensing circuit of *E. coli*. EnvZ is a bifunctional SHK that phosphorylates and
590 dephosphorylates its cognate RR, OmpR. Osmotic pressure (Osm), depicted in red, due to the
591 presence of small inner membrane-impermeable solutes, alters the ratio of these activities resulting
592 in a net increase of intracellular OmpR-P. The intracellular level of OmpR-P governs transcription
593 of *ompF* (yellow) and *ompC* (blue) and was monitored by employing an *E. coli* strain that contains
594 a transcriptional fusion of *yfp* to *ompF* and of *cfp* to *ompC*. Intracellular levels of OmpR-P were
595 estimated by calculating the CFP/YFP ratio (red). The gray-filled circles on the dashed lines
596 indicate the estimated OmpR-P levels in cells expressing one of the aromatically tuned variants at
597 intermediate levels. Aromatic tuning in EnvZ resulted in a pattern of signal output that did not
598 correlate with the vertical position of the aromatic residues but appeared more helical in distribution
599 suggesting that the surface of TM2 that the residues were located upon was of greater importance
600 [2].

601

602 Figure 2. Minimum glycosylation distance (MGD) analysis of Tar and EnvZ TM2. (A) Linear and
603 topological characteristics of the model Lep protein used in this study. The model protein contains a
604 glycosylation-accepting site (G1) more than 20 residues away from the luminal boundary TM1 and
605 a second glycosylation-accepting site (G2) that is positioned between 6 and 11 residues ($d = 6$ to d
606 $= 11$) from the boundary of TM2. If TM2 is displaced, the position of the second G2 relative to the
607 boundary of the membrane will change and allow a previously unglycosylated accepting site (red)
608 to become glycosylated (green). It is also possible to monitor displacements of TM2 into the
609 membrane. (B) Primary sequence of TM2s used for glycosylation-mapping analysis. A motif
610 commonly found in transmembrane helices consisting of flanking positively charged residues

611 (blue), adjacent aromatic residues (red) and an aliphatic core (uncolored) was present in both
612 segments. The flanking Gly-Pro-Gly-Gly tetrapeptide was included to reduce the propensity for
613 formation of secondary structure. The first Gly of the flanking tetrapeptide (G_{+1}) is considered the
614 first residue ($d = 1$) outside of TM2. MGD values for each segment are provided above the primary
615 sequence. (C) Identification and analysis of the different species by SDS-PAGE. The presence of
616 rough microsomes (RM) facilitates glycosylation due to the presence of oligosaccharyltransferase
617 (OST). Differences in migration allow identification of the unglycosylated (single white dot), singly
618 glycosylated (G1 only; single gray dot) and the doubly glycosylated moieties (G1 and G2; two gray
619 dots). An increase in the doubly glycosylated moiety is observed as G2 is moved further away from
620 the boundary of TM2 from Tar. MGD is calculated as the number of residues (d) required to
621 achieve 40% double glycosylation (dashed line). The MGD for Tar TM2 was found to be 8.3. (D) A
622 similar analysis was performed with EnvZ TM2 and a value of 8.6 was determined for the MGD
623 (dashed line).

624

625 Figure 3. Glycosylation-mapping analysis of aromatically tuned Tar TM2 segments. (A) Primary
626 sequence of the C-terminal end of Tar TM2. Within the segment, a Trp-Tyr tandem was moved
627 (red). MGD values are provided above the primary sequence of each segment. (B) As described in
628 Figure 2C, the amount of the doubly glycosylated moiety correlates with the number of residues
629 between the end of TM2 and G2. Results are provided for the modified TM2 segments from Tar: -3
630 variants as filled circles; -2 variants as filled squares; -1 variants as filled diamonds; +1 variants as
631 filled downward-pointing triangles; +2 variants as filled upward-pointing triangles; and +3 variants
632 as filled leftward-pointing triangles. The red line indicates results for receptors containing the
633 aromatic residues at their original position. MGDs were determined via the dashed lines.

634

635 Figure 4. Glycosylation-mapping analysis of aromatically tuned EnvZ TM2 segments. (A) Primary
636 sequence of the C-terminal end of EnvZ TM2. Within the segment, a Trp-Leu-Phe triplet was
637 moved (red). MGD values are provided above the primary sequence of each segment. ND indicates
638 that the MGD was not determined. (B) As described in Figure 2C, the amount of the doubly
639 glycosylated moiety correlates with the number of residues between the end of TM2 and G2.
640 Results are provided for the modified TM2 segments from EnvZ: -3 variants as filled circles; -2
641 variants as filled squares; -1 variants as filled diamonds; +1 variants as filled downward-pointing
642 triangles; and +2 variants as filled upward-pointing triangles. The red line indicates results for the
643 receptor containing the aromatic residues at their original position. MGDs were calculated via the
644 dashed lines.

645

646 Figure 5. Proposed model for the large difference in MGD values for the WLF-3 and WLF-2
647 variants of EnvZ. We propose that the baseline position of EnvZ TM2 (WLF 0) is due to both the
648 interaction of Trp-176 with the polar/hydrophobic interfacial region and due to snorkeling of the
649 Arg-180 side chain to interact with the negatively charged phospholipids (left). One possibility for
650 the large change in MGD observed between WLF-3 (7.9) and WLF-2 (8.4) is that upon moving the
651 Trp into the membrane at residue position 173, TM2 is displaced out of the membrane to such an
652 extent that the Arg residue at residue position 180 can no longer snorkel and interact with the
653 negatively charged lipids (center). When the Trp residue is moved one more step toward the
654 interface, *i.e.* at position 174, the side chain or the Arg residue is in a position where it could still
655 interact with the membrane surface (right).

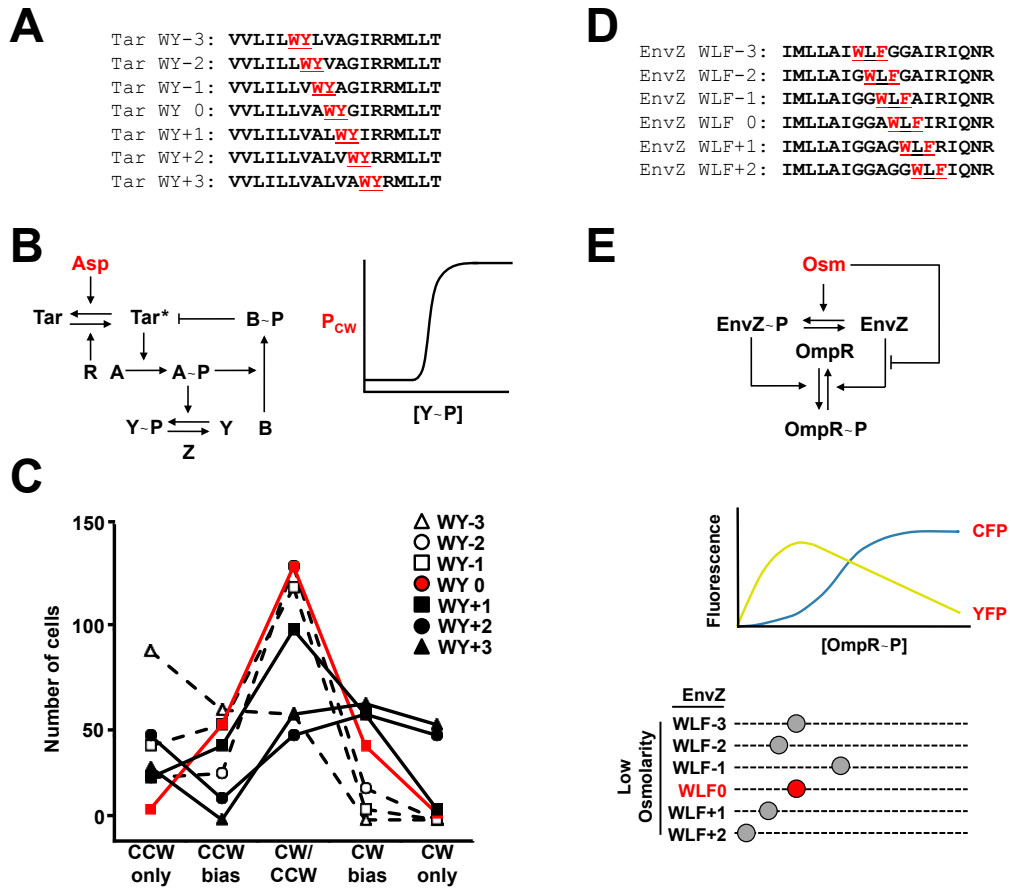


Figure 1.

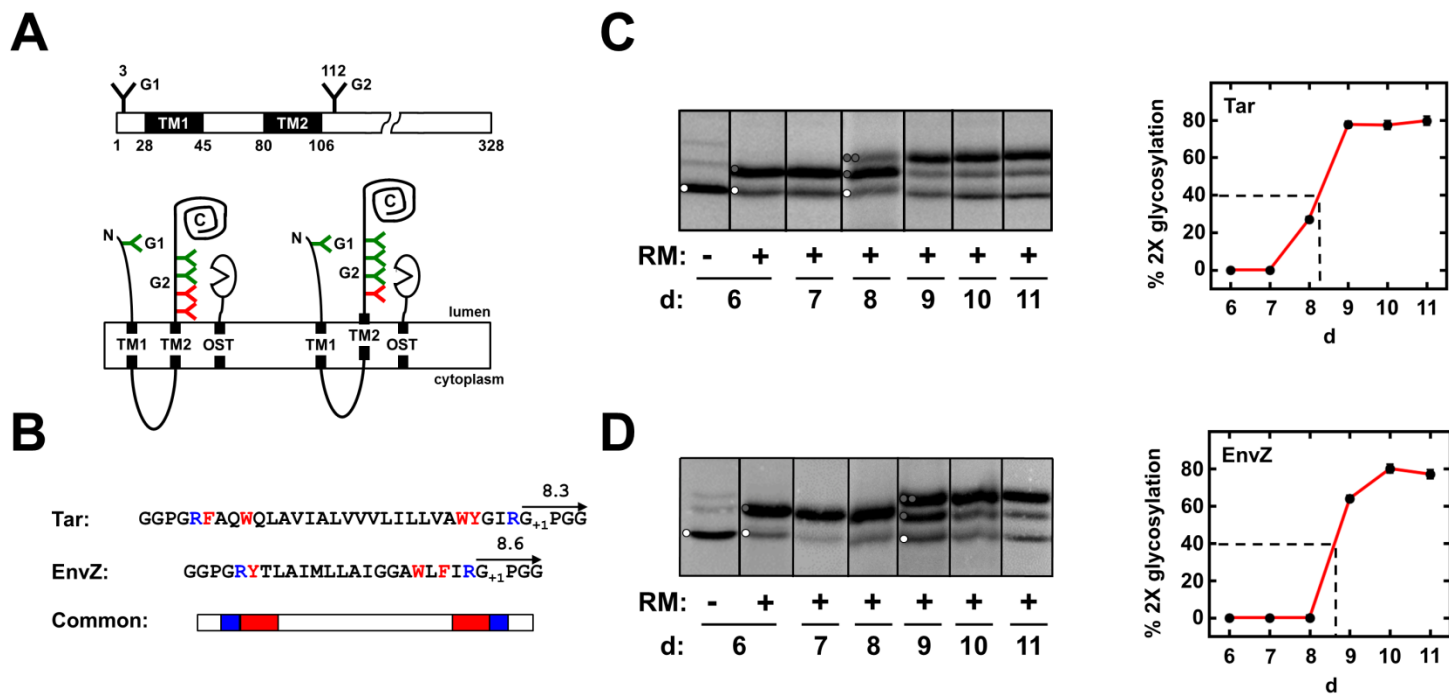


Figure 2.

A

Tar WY-3: VVLILLWYLVAGIRG₊₁PGG $\xrightarrow{8.2}$

Tar WY-2: VVLILLWYVAGIRG₊₁PGG $\xrightarrow{8.2}$

Tar WY-1: VVLILLVWYAGIRG₊₁PGG $\xrightarrow{8.2}$

Tar WY 0: VVLILLVAWYGIRG₊₁PGG $\xrightarrow{8.3}$

Tar WY+1: VVLILLVALWYIRG₊₁PGG $\xrightarrow{8.6}$

Tar WY+2: VVLILLVALVWYRG₊₁PGG $\xrightarrow{8.6}$

Tar WY+3: VVLILLVALVAWYG₊₁PGG $\xrightarrow{8.7}$

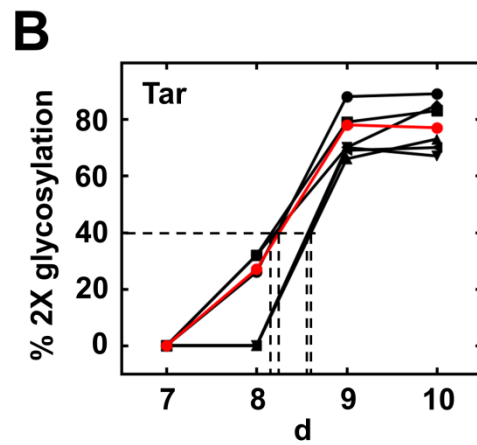


Figure 3.

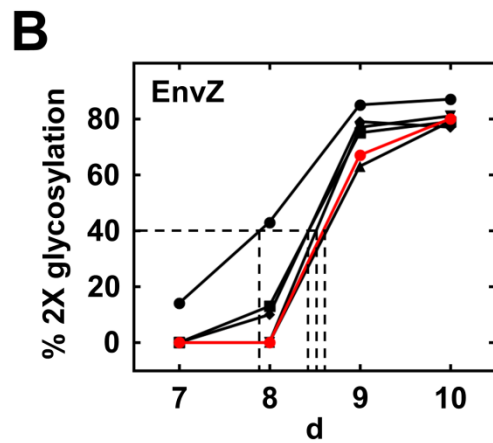
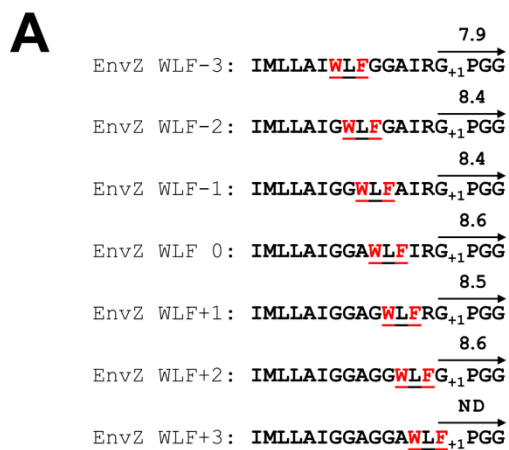


Figure 4.

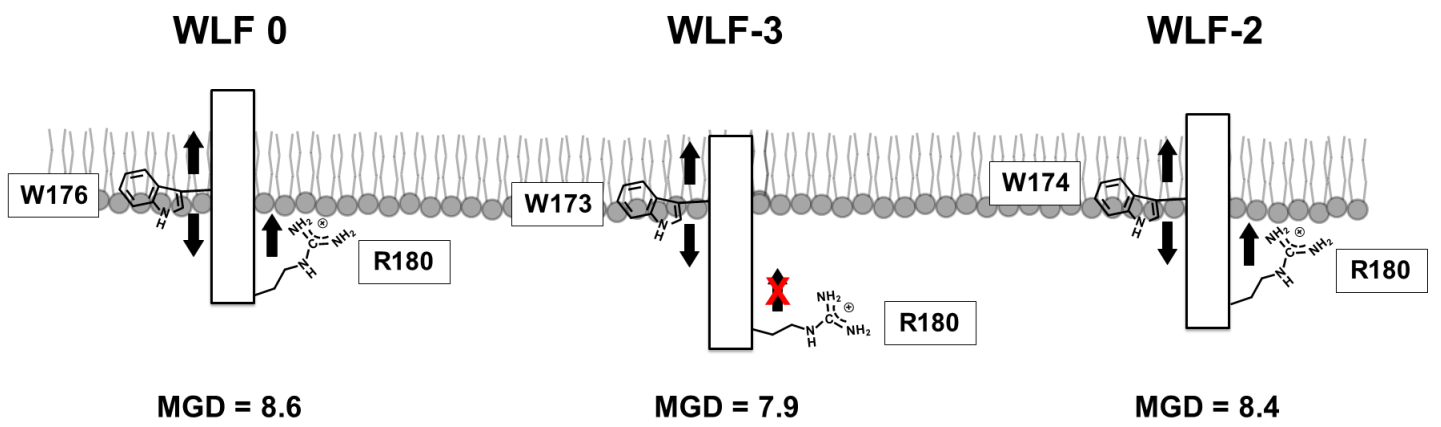


Figure 5.